Characterization of Chemical Processes in Non-thermal Plasmas for the Destruction of Volatile Organic Compounds

David S. Green, L. Wayne Sieck, and John T. Herron

Chemical Kinetics and Thermodynamics Division, Chemical Science and Technology Laboratory, National Institute of Standards and Technology, Gaithersburg, MD 20899

The nature of chemical mechanisms in the degradation of toluene in dilute air and nitrogen plasma streams has been investigated both theoretically and experimentally. The study focuses on processes subsequent to the initiating electron-molecule collisions, and on the role of water vapor in determining the final products. The computational model consists of a select set of ion and neutral kinetics and predicts the temporal rise and fall in species' concentration. Evolution of the ion-neutral interactions is probed experimentally using pulsed e-beam high-pressure mass spectrometry.

Detailed chemical processes in non-thermal plasma devices need to be fully characterized so that kinetic models can predict the destruction efficiency of volatile organic compounds (VOCs) in the plasma environments as a function of changing gas stream conditions. The starting point for modeling the treatment of toluene (T) was guided by the mechanism developed by Mätzing [1] for the e-beam treatment of flue gases for SO_x and NO_x removal. The reaction sequence was modeled and calculated using the Acuchem program [2] and a subset of the important reactions and rate constants are listed in Table 1. This is not intended to be a complete mechanism; the product chemistry from reactions of toluene with OH, neutralization reactions, and reactions incorporating ion and neutral products into aerosols are not included. Figs. 1 and 2 show the temporal profiles predicted for selected ion and neutral species.

As can be seen from Figs. 1 and 2, the concentration of ions H_3O^+OH and $O_2^+H_2O$ rise and fall on a very short time scale (< 0.02 μs). Fig. 1 also shows that within the first 0.02 μs the rising profiles of OH, $H_3O^+H_2O$, and protonated toluene ion TH^+ track each other very closely. The scaling factors indicate that OH and $H_3O^+H_2O$ are of nearly identical concentration and in greater abundance than the TH^+. Fig. 2, indicates an initial slow and steady decrease in T and rise in T^+. However, when the modeling runs are carried out to reaction times as long as 1 ms, we find that the OH is essentially all consumed and T is significantly removed, while $H_3O^+H_2O$, TH^+, and

T^+, in the absence of loss processes, remain at the limiting values shown in Figs. 1 and 2. These predictions are consistent with the destruction of T resulting dominantly from chemical attack by OH. Fig. 2 also shows that the source of the toluene ion T^+, aside from processes occurring in the first 0.02 μs, is charge exchange of T with NO^+. A more complete model would need to include interactions and clustering of NO^+ with H_2O which would modify the NO^+ and hence T^+ profiles.

Table 1. Reactions included in the model.

	Process [a]	Rate Constant [b]		Process [a]	Rate Constant [b]
1.	$N_2^+ + O_2 \rightarrow O_2^+ + N_2$	4.8e-11	29.	$O_2^+ + N \rightarrow NO^+ + O$	1.8e-10
2.	$N_2^+ + O_2 \rightarrow NO^+ + NO$	1e-17	30.	$O_2^+ + O_2 \rightarrow O_4^+$	7.6e-11
3.	$N_2^+ + NO \rightarrow NO^+ + N_2$	3.3e-10	31.	$O^+ + N_2 \rightarrow N_2^+ + O$	1.7e-12
4.	$N_2^+ + NO_2 \rightarrow NO_2^+ + N_2$	3e-10	32.	$O^+ + N_2 \rightarrow NO^+ + N$	1.5e-9
5.	$N_2^+ + O_3 \rightarrow O_2^+ + O + N_2$	1e-10	33.	$O^+ + O_2 \rightarrow O_2^+ + O$	2.9e-11
6.	$N_2^+ + O \rightarrow NO^+ + N$	1.4e-10	34.	$O^+ + NO \rightarrow NO^+ + O$	1e-12
7.	$N_2^+ + O \rightarrow NO^+ + N$	1.8e-10	35.	$O^+ + NO_2 \rightarrow NO_2^+ + O$	1.6e-9
8.	$N_2^+ + O \rightarrow O^+ + N_2$	6e-12	36.	$O^+ + NO_2 \rightarrow NO^+ + O_2$	5e-10
9.	$N_2^+ + N \rightarrow N^+ + N_2$	1e-11	37.	$O^+ + O_3 \rightarrow O_2^+ + O_2$	1.1e-10
10.	$N_2^+ + N \rightarrow N_3^+$	2.7e-10	38.	$O_4^+ + NO \rightarrow NO^+ + 2O_2$	5e-10
11.	$N_2^+ + N_2 \rightarrow N_4^+$	1.4e-9	39.	$O_4^+ + NO_2 \rightarrow NO_2^+ + 2O_2$	3e-10
12.	$N^+ + O_2 \rightarrow NO^+ + O$	2.6e-10	40.	$O_4^+ + O \rightarrow O_2^+ + O_3$	3e-10
13.	$N^+ + O_2 \rightarrow N + O_2^+$	3e-10	41.	$N_4^+ + O_2 \rightarrow O_2^+ + 2N_2$	2.5e-10
14.	$N^+ + O_2 \rightarrow O^+ + NO$	3.6e-11	42.	$O_4^+ + H_2O \rightarrow O_2^+H_2O + O_2$	2e-9
15.	$N^+ + NO \rightarrow NO^+ + N$	4.1e-10	43.	$O_2^+H_2O + H_2O \rightarrow H_3O^+OH + O_2$	2e-9
16.	$N^+ + NO \rightarrow N_2^+ + O$	5e-11	44.	$H_3O^+OH + H_2O \rightarrow H_3O^+H_2O + OH$	2e-9
17.	$N^+ + NO_2 \rightarrow NO_2^+ + N$	3e-10	45.	$T + N_4^+ \rightarrow T^+ + 2N_2$	2e-9
18.	$N^+ + O_3 \rightarrow NO^+ + O_2$	5e-10	46.	$T + O_2^+ \rightarrow T^+ + O_2$	2e-9
19.	$N^+ + O \rightarrow O^+ + N$	1e-12	47.	$T + O_4^+ \rightarrow T^+ + 2O_2$	2e-9
20.	$N^+ + O \rightarrow NO^+$	2.7e-10	48.	$T + O_2^+H_2O \rightarrow T^+H_2O + O_2$	2e-9
21.	$N^+ + N \rightarrow N_2^+$	2.7e-10	49.	$T + H_3O^+OH \rightarrow TH^+ + OH + H_2O$	2e-9
22.	$N^+ + N_2 \rightarrow N_3^+$	4.9e-10	50.	$T + OH \rightarrow P$	5.2e-12
23.	$N_3^+ + O_2 \rightarrow NO^+ + O + N_2$	1e-10	51.	$T + N_3^+ \rightarrow T^+ + N + N_2$	2e-9
24.	$N_3^+ + NO \rightarrow NO^+ + N + N_2$	1e-10	52.	$T + NO^+ \rightarrow T^+ + NO$	2e-9
25.	$N_3^+ + N \rightarrow N_2^+ + N_2$	1e-10	53.	$T + NO_2^+ \rightarrow T^+ + NO_2$	2e-9
26.	$O_2^+ + N_2 \rightarrow NO^+ + NO$	1e-16	54.	$O + O_2 \rightarrow O_3$	1.6e-14
27.	$O_2^+ + NO \rightarrow NO^+ + O_2$	3.5e-10	55.	$N + O_3 \rightarrow NO + O_2$	1e-16
28.	$O_2^+ + NO_2 \rightarrow NO_2^+ + O_2$	6e-10	56.	$NO + O_3 \rightarrow NO_2 + O_2$	1.8e-14

a. Reactions pertaining to toluene are indicated by $T \equiv C_7H_8$, $T^+ \equiv C_7H_8^+$, $TH \equiv C_7H_9^+$, P≡products.

b. Rate constants are adopted from standard data compilations or estimated from the appropriate ion collision rate. All rate constants have units of $cm^3 molecule^{-1} s^{-1}$.

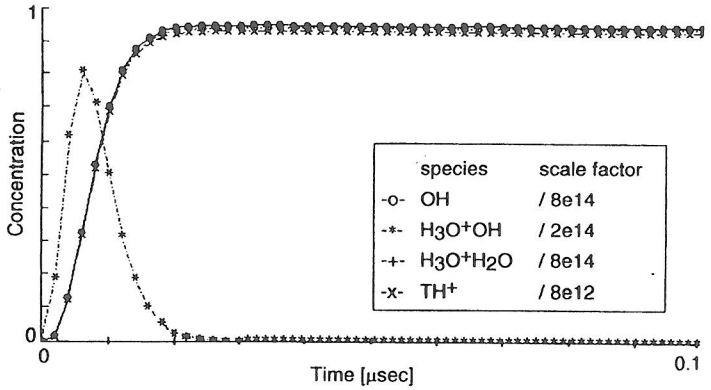

Fig. 1 Temporal behavior of OH, H_3O^+OH, $H_3O^+H_2O$, and TH^+ for a model of the toluene-air plasma. Initial conditions: total pressure, 1 bar; temperature, 300K; ion concentrations, O^+ = 2.2e14, O_2^+ = 3.7e14, N^+ = 1.2e14, and N_2^+ = 4.04e14 molecule/cm^3, neutral concentrations, toluene = 2.7e15 and water = 2.7e17 molecule/cm^3. Total reaction time, 10^{-7} s.

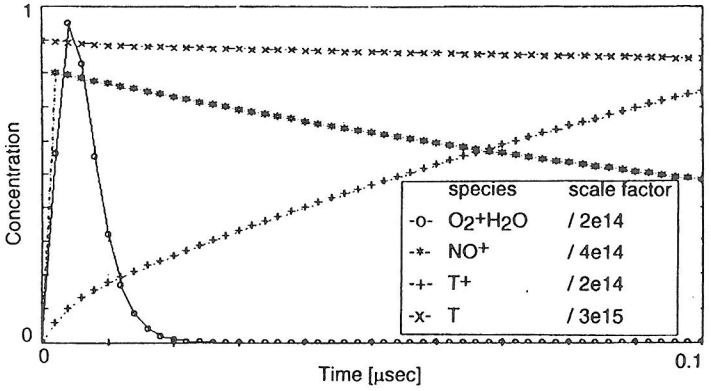

Fig. 2 Temporal behavior of $O_2^+H_2O$, NO^+, T^+, and T for a model of the toluene-air plasma. Initial conditions: total pressure, 1 bar; temperature, 300K; ion concentrations, O^+ = 2.2e14, O_2^+ = 3.7e14, N^+ =1.2e14, and N_2^+ = 4.04e14 molecule/cm^3, neutral concentrations, toluene = 2.7e15 and water = 2.7e17 molecule/cm^3. Total reaction time, 10^{-7} s.

Experiments have been conducted to validate and advance the predictive kinetic and mechanistic models. Pulsed e-beam with high-pressure mass spectrometry has been exploited to make direct measurements of equilibrium ion distributions and to map temporal profiles of species' concentration. A schematic of the experimental system is shown in Fig. 3. The pulsed high-pressure mass spectrometry technique [3] is a powerful tool for characterizing thermochemistry of ion-molecule process and provides data on the terminal equilibrium of ion species prior to neutralization. A primary goal has been to study the effect of water vapor levels and cluster formation on the final products from plasma degradation of toluene in humid air and nitrogen mixtures. The spectrometer operates at pressures up to 0.7 Pa (5 Torr), and is temperature controlled using cartridge heaters which operate over the range of 300 to 700 K. The electron beam is modulated to intersect the ionization region and provide a 1 ms pulse width at energies of 500 to 1000 eV. There are no potential gradients within the reaction volume, and all ions are in thermal equilibrium with the bulk carrier gas (air or N_2 in the present case) at any chosen temperature. Ion residence times in the reaction volume were about 10 ms. The levels of humidity were varied widely, starting with no added water and increasing to almost 2 % added water. Fig. 4 shows the ion signal intensity as a function of added water.

The experimental results confirm the role of water vapor in generating OH which as the primary species for destroying toluene and determining the terminal ion distribution. The measurements support the predicted rise in $H_3O^+H_2O$ and OH as given in reaction 44 of Table 1. Similarly, the model prediction of short term intermediates $O_2^+H_2O$ and H_3O^+OH via reactions 43 and 44 is consistent with the absence of these species in the mass spectrum.

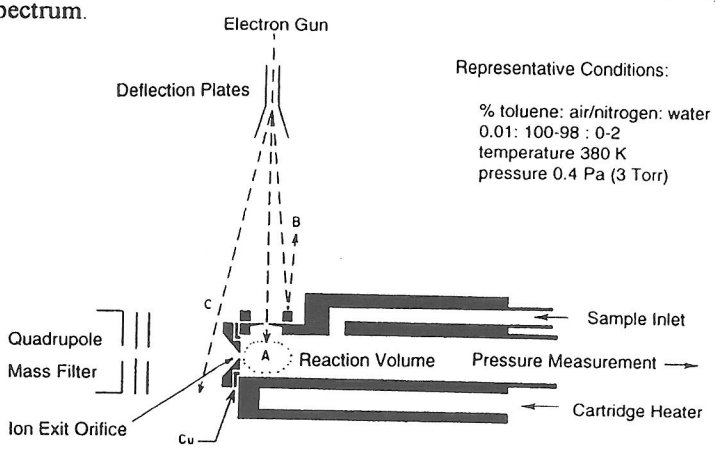

Fig. 3. Schematic of the NIST pulsed electron-beam high-pressure mass spectrometer ion source along the main axis. Position A shows the path of the electron beam to effect ionization in the reaction volume, position B is the path during the non-ionizing path of the cycle, and position C is for calibration.

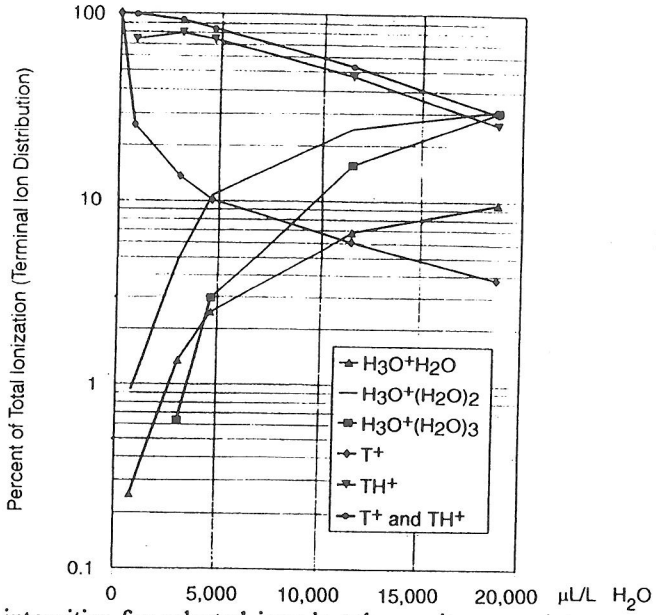

Fig. 4. Ion intensities for selected ions in toluene-nitrogen mixtures as a function of water. Conditions: total pressure, 0.4 Pa (3 Torr); toluene, 124 μL/L (ppm); temperature, 380 K. Ion concentrations are normalized to percent of total ionization, and correspond to the terminal distribution of ionic end-products.

The experiments suggest that the generation of water clusters provides a competing channel which shields the generation of T^+ and TH^+. At short time both T^+ and TH^+ rise in concentration to nearly the same magnitude. While TH^+ rises and remains fixed in the model, the experiments reveal an abundance of TH^+ which is only diminished by a factor of 2 with rise in water clusters over the range shown in Fig. 4. By contrast, the concentration of T^+ decreases by an order of magnitude with increase in percentage of water over the same range. The ion chemistry involving the generation and reactions of protonated water clusters in air-toluene mixtures is very complex, and is currently the focus of the experimental program in this laboratory.

Acknowledgments: Support from the Strategic Environmental Research and Development Program (SERDP) is gratefully acknowledged. We also wish to acknowledge the useful discussions and contributions of Dr. Andrzej Miziolek, U.S. Army Research Laboratory, Aberdeen Proving Ground, Maryland.

References

1. Mätzing, H., Adv. Chem. Phys., Vol. LXXX, pp. 315-402 (1991).
2. Mautner, M. and Sieck, L.W., J. Am. Chem. Soc. 113, 4448 (1991).
3. Braun, W., Herron, J.T., and Kahaner, D., Int. J. Chem. Kin. 20, 51 (1988).